


1,2,3-Triazole-linked 5-benzylidene (thio)barbiturates as novel tyrosinase inhibitors and free-radical scavengers

Sara Ranjbar¹ | Parisa-sadat Shahvaran² | Najmeh Edraki³ |
 Mahsima Khoshneviszadeh³ | Mahdiah Darroudi⁴ | Yaghoub Sarrafi⁴ |
 Mahshid Hamzehlouei⁵ | Mehdi Khoshneviszadeh^{2,3} 

¹Pharmaceutical Sciences Research Center, Shiraz University of Medical Sciences, Shiraz, Iran

²Department of Medicinal Chemistry, School of Pharmacy, Shiraz University of Medical Sciences, Shiraz, Iran

³Medicinal and Natural Products Chemistry Research Center, Shiraz University of Medical Sciences, Shiraz, Iran

⁴Department of Organic Chemistry, Faculty of Chemistry, University of Mazandaran, Babolsar, Iran

⁵Department of Chemistry, Jouybar Branch, Islamic Azad University, Jouybar, Iran

Correspondence

Mehdi Khoshneviszadeh, Department of Medicinal Chemistry, School of Pharmacy, Shiraz University of Medical Sciences, PO Box 71345-3388, Shiraz, Iran.
 Email: m.khoshneviszadeh@gmail.com

Funding information

Vice-Chancellor for Research, Shiraz University of Medical Sciences, Iran, Grant/Award Numbers: 95-01-103-12178, 98-01-36-20126

Abstract

In this study, benzyl-1,2,3-triazole-linked 5-benzylidene (thio)barbiturate derivatives **7a-d** and **8a-h** were designed as potential tyrosinase inhibitors and free-radical scavengers. The twelve derivatives were synthesized *via* the [3+2] cycloaddition reaction of the corresponding benzyl azide as a dipole and the corresponding alkyne as a dipolarophile in the presence of copper(I) species, generated *in situ* from copper (II)/ascorbate. The thiobarbiturate derivative **8h** and the barbiturate derivative **8b** bearing 4-fluoro and 4-bromo groups on the benzyl-triazole moiety were found to be the most potent tyrosinase inhibitors with IC₅₀ values of 24.6 ± 0.9 and 26.8 ± 0.8 μM, respectively. Almost all the compounds showed a good radical scavenging activity with EC₅₀ values in the range of 29.9–324.9 μM. Derivatives **7a**, **8f**, and **8h** were the most potent free-radical scavengers with EC₅₀ values of 29.9 ± 0.8, 36.8 ± 0.9, and 39.2 ± 1.1 μM, respectively. The kinetic analysis revealed that compound **8h** was a mixed-type tyrosinase inhibitor. The molecular docking analysis indicated that **8b** and **8h** were well accommodated in the active site of the tyrosinase enzyme and possessed the most negative binding energy values of –8.55 and –8.81 kcal/mol, respectively. Moreover, it was found that the two residues, Asn81 and Glu322, played a significant role in forming stable enzyme-inhibitor complexes.

KEYWORDS

antioxidant, barbituric acid, diphenolase activity, docking, kojic acid, triazole

1 | INTRODUCTION

Tyrosinase (EC 1.14.18.1) is a copper-containing oxidase enzyme distributed widely in nature. It is a rate-limiting enzyme that contributes to melanin biosynthesis by catalyzing the two consecutive oxidation steps of L-tyrosine.^[1] Initially, tyrosinase interacts with L-tyrosine to produce 3,4-dihydroxy-L-phenylalanine (L-DOPA; monophenolase activity), and in the second step, the enzyme catalyzes the oxidation of L-DOPA to dopaquinone (diphenolase activity).^[2] Dopaquinone is a reactive substance that can polymerize

to generate melanin; hence, tyrosinase has a crucial role in melanogenesis and many tyrosinase inhibitors have been developed for the remedy of hyperpigmentation-related skin disorders, such as melasma, freckles, ephelides, and senile lentigines.^[3,4] Tyrosinase is also associated with neurodegenerative disorders including Parkinson's and Huntington's diseases, as the excessive formation of dopaquinone in the brain results in neuronal damage and cell death.^[5] Moreover, tyrosinase plays an important role in enzymatic browning of fruits and vegetables, which leads to fast degradation during the postharvest and handling processes.^[6] Therefore, tyrosinase is an

evolving target in the fields of medicine, cosmetics, agriculture, and food industry, and several natural and synthetic tyrosinase inhibitors, including hydroquinone, ascorbic acid derivatives, azelaic acid, retinoids, arbutin, kojic acid, resveratrol, and polyphenolic compounds, have been applied.^[4] However, some common tyrosinase inhibitors, such as hydroquinone, kojic acid, and arbutin, have been reported to cause undesirable side effects, including dermatitis, cytotoxicity, and carcinogenicity.^[4,7,8] Besides, tyrosinase inhibitors have some limitations such as low efficacy, poor bioavailability, and instability during storage, and they can also cause off-flavor, off-donor, and allergic reactions.^[4,9] Therefore, the identification and development of new, effective, and safe tyrosinase inhibitors with drug-like properties are greatly needed.

Barbituric acid and its derivatives have attracted the attention of scientists due to their therapeutic importance. Barbiturates have exhibited various biological activities such as antibacterial,^[10,11] sedative, hypnotic,^[12,13] antispasmodic,^[14] anticonvulsant,^[15] anticancer,^[16,17] anti-inflammatory,^[18] antiurease,^[19] antitubercular,^[20] and antioxidant^[21] ones. It is also reported that some arylidene barbiturates are potent tyrosinase inhibitors.^[22–24] Also, the 1,2,3-triazole heterocyclic nucleus has emerged as a versatile pharmacophore due to its potency to establish hydrogen bonding and dipole–dipole interactions that have made it very stable to hydrolysis and oxidative/reductive conditions.^[25] 1,2,3-Triazole-containing compounds have shown a broad range of biological activities such as anticancer,^[26] antibacterial,^[27] anti-inflammatory,^[28] antifungal,^[29] antitubercular,^[30] antiacetylcholinesterase,^[31] and antityrosinase activities.^[32,33]

Considering the above-mentioned pharmacophores, 1,2,3-triazole-linked 5-benzylidene (thio)barbiturates were designed and synthesized

as tyrosinase inhibitors. The synthesized compounds were screened for tyrosinase inhibitory and antioxidant (radical scavenging) activities. The inhibition kinetic analysis was carried out for the most potent derivative. Moreover, to gain some information on the ligand–receptor interactions, a molecular docking analysis was performed.

2 | RESULTS AND DISCUSSION

2.1 | Design approach

The structure of target benzyl-1,2,3-triazole-linked 5-benzylidene (thio)barbiturates was designed by applying a molecular hybridization strategy based on the structures of some potent tyrosinase inhibitors, as reported in the literature (Figure 1). It has been reported that hydroxyl/methoxy-substituted 5-benzylidene (thio)barbiturates exhibited a tyrosinase inhibitory activity ($IC_{50} = 1.50\text{--}100.0\text{ }\mu\text{M}$). Benzylidene barbiturate and benzylidene thiobarbiturate derivatives bearing 4-methoxy function possessed IC_{50} values of 100.0 and 70.1 μM , respectively (Figure 1a).^[23] Moreover, Khan et al.^[34] introduced a series of 5-benzylidene barbiturates containing different substitutions on benzylidene moiety as a class of DPPH (2,2-diphenyl-1-picrylhydrazyl) radical scavengers with IC_{50} values in the range of 6.2–406.7 μM . In our previous study, we proved that some phthalimide–1,2,3-triazole (Figure 1b) hybrid structures were potent tyrosinase inhibitors.^[32] On the basis of these findings, 5-benzylidene (thio)barbiturate–1,2,3-triazole hybrids bearing different benzyl moieties were designed (Figure 1).

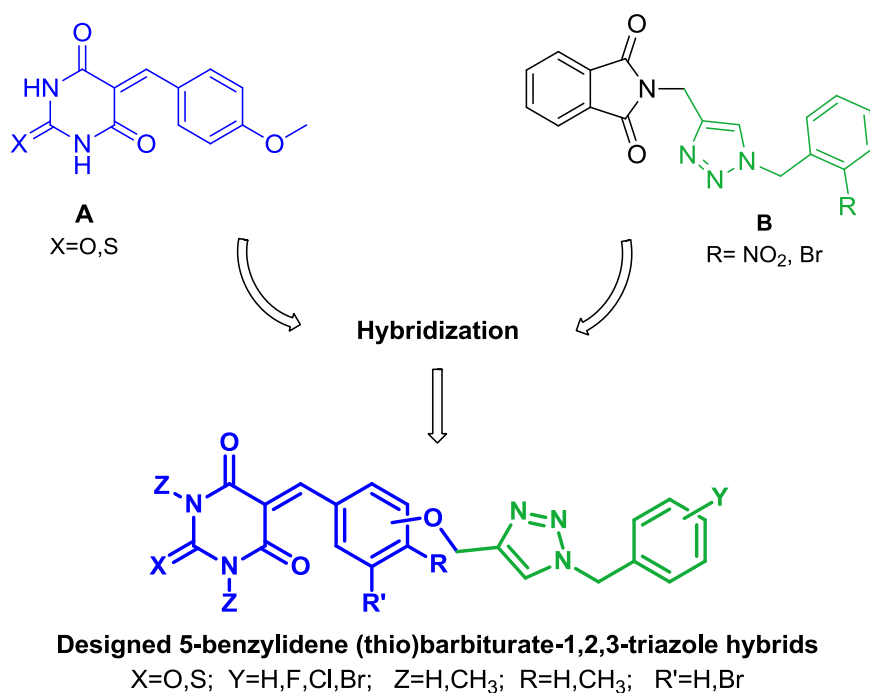


FIGURE 1 The design of proposed tyrosinase inhibitors using the molecular hybridization approach

2.2 | Chemistry

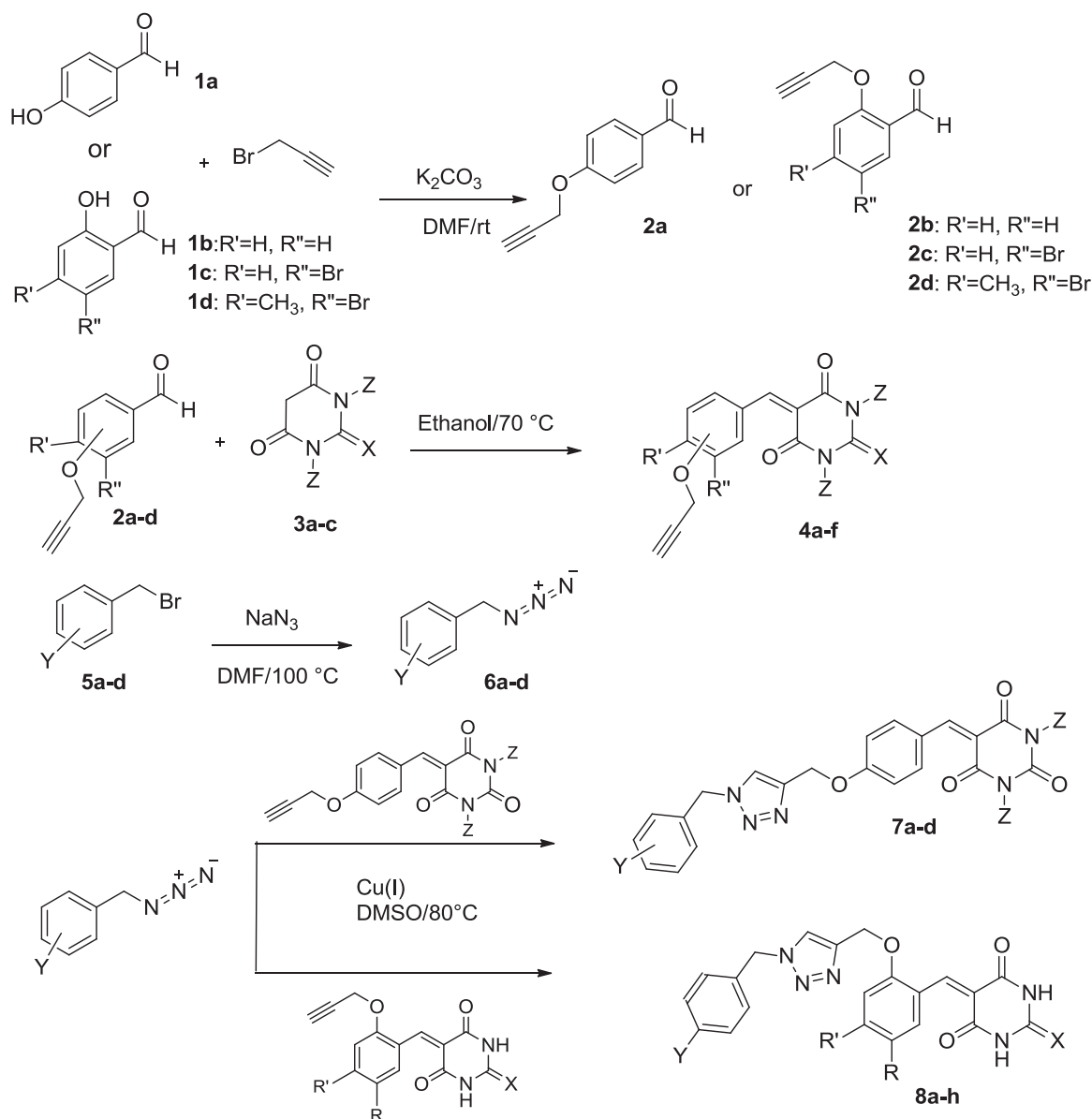
The procedure for the synthesis of 1,2,3-triazole-linked 5-benzylidene (thio)barbiturates (**7a–d** and **8a–h**) is illustrated in Scheme 1. Initially, 2-(prop-2-yn-1-yloxy)benzaldehyde (**2a**), 4-(prop-2-yn-1-yloxy)benzaldehyde (**2b**), 5-bromo-2-(prop-2-yn-1-yloxy)benzaldehyde (**2c**), and 5-bromo-4-methyl-2-(prop-2-yn-1-yloxy)benzaldehyde (**2d**) were synthesized from the reaction of the corresponding hydroxybenzaldehyde (**1a–d**) and propargyl bromide in the presence of K_2CO_3 . Then, the alkynes **4a–f** were acquired through the Knoevenagel condensation of the related (thio)barbituric derivative (**3a–c**) and corresponding propargylated hydroxybenzaldehyde (**2a–d**) under reflux conditions in good yields. The reaction of different benzyl bromides **5a–d** and sodium azide in dimethylformamide (DMF) at 100°C afforded organic azides **6a–d**.

Finally, the cycloadducts **7** and **8** were obtained from the [3+2] cycloaddition reaction of the corresponding benzyl azide (**6a–d**) as a dipole and the corresponding alkyne (**4a–f**) as a dipolarophile in the presence of copper(I) species, generated in situ from copper(II)/ascorbate in dimethyl sulfoxide (DMSO).

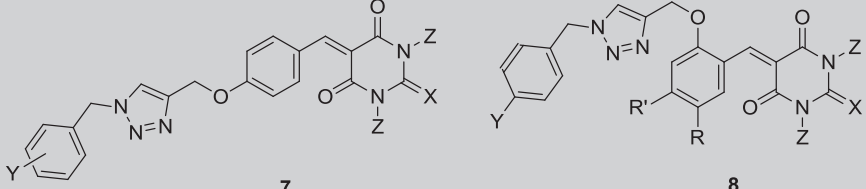
2.3 | Biological activity

2.3.1 | Mushroom tyrosinase inhibitory activity

Synthesized compounds were screened for their potential inhibitory effect on the diphenolase activity of mushroom tyrosinase. According to the IC_{50} values listed in Table 1, thiobarbiturate derivative **8h** and barbiturate derivative **8b** were the most potent tyrosinase inhibitors



SCHEME 1 The synthesis of 1,2,3-triazole-linked 5-benzylidene (thio)barbiturates. DMF, dimethylformamide; DMSO, dimethyl sulfoxide

TABLE 1 The tyrosinase inhibitory activity and free-radical scavenging potential of synthesized compounds


Compounds	X	R	R'	Y	Tyrosinase inhibitory activity ^a Z	DPPH radical scavenging activity ^a IC ₅₀ (μM) ^b	EC ₅₀ (μM)
7a	O	-	-	2-Cl	H	>50	29.9 ± 0.8
7b	O	-	-	4-Br	H	>50	>100
7c	O	-	-	H	CH ₃	>50	134.3 ± 2.3
7d	O	-	-	4-F	CH ₃	>50	67.8 ± 0.7
8a	O	H	H	H	H	49.1 ± 2.2	1,000.1 ± 3.6
8b	O	H	H	4-Br	H	26.8 ± 0.8	239.6 ± 1.5
8c	O	H	Br	4-F	H	>50	324.9 ± 2.8
8d	S	H	H	H	H	44.4 ± 0.4	74.8 ± 0.6
8e	S	H	H	4-Br	H	44.2 ± 1.3	195.0 ± 3.5
8f	S	H	H	4-F	H	>50	36.8 ± 0.9
8g	S	CH ₃	Br	H	H	>50	122.1 ± 2.4
8h	S	CH ₃	Br	4-F	H	24.6 ± 0.9	39.2 ± 1.1
Kojic acid	-	-	-	-	-	16.5 ± 0.3	-
Quercetin	-	-	-	-	-	-	9.4 ± 0.6

Abbreviation: DPPH, 2,2-diphenyl-1-picrylhydrazyl.

^aValues represent means ± standard error of three to four independent experiments.

^b50% inhibitory concentration (IC₅₀).

with IC₅₀ values of 24.6 ± 0.9 and 26.8 ± 0.8 μM, respectively. Compounds **8a**, **8d**, and **8e** demonstrated a moderate tyrosinase inhibitory activity with IC₅₀ values in the range of 44.2–49.1 μM. In general, Group **8** compounds containing benzyl-triazolyl-methoxy substitutions at the *ortho* position of 5-benzylidene (thio)barbiturate moiety showed a superior inhibitory activity on tyrosinase than Group **7** compounds bearing benzyl-triazolyl-methoxy groups at the *para* position. It seems that substitutions on the benzyl ring have no considerable effect on the inhibitory potential of Class **7** compounds; however, this does not apply to Group **8** compounds. Interestingly, introducing a 4-Br function on the benzyl core of Group **8** barbiturates, as in **8b**, led to a remarkable increase in the activity as compared with **8a** (IC₅₀ = 49.1 ± 2.2 μM). Changing the barbiturate ring in compound **8b** to thiobarbiturate, as in compound **8e** (IC₅₀ = 44.2 ± 1.3 μM), reduced the tyrosinase inhibitory activity. However, replacing 4-Br with 4-F in the case of thiobarbiturate **8h** (IC₅₀ = 24.6 ± 0.9) improved the inhibitory potential.

It can be stated that benzyl-1,2,3-triazole-linked 5-benzylidene (thio)barbiturate derivatives **8h** and **8b** (IC₅₀ = 24.6 ± 0.9 and 26.8 ± 0.8 μM, respectively) were better tyrosinase inhibitors than (thio)barbituric acid (IC₅₀ = >200 μM) and 4-methoxybenzylidene

(thio)barbiturate (IC₅₀ = 70.1–100.0 μM); however, most of the hydroxyl-substituted benzylidene (thio)barbiturates (IC₅₀ = 1.5–17.1 μM) were more effective inhibitors than compounds **8h** and **8b**.^[23,24]

2.3.2 | Free-radical scavenging activity

All the compounds except **8a** exhibited a good radical scavenging activity with EC₅₀ values in the range of 29.9–324.9 μM (Table 1). Compounds **7a**, **8f**, and **8h** were the most potent free-radical scavengers with EC₅₀ values of 29.9 ± 0.8, 36.8 ± 0.9, and 39.2 ± 1.1 μM, respectively. Derivatives **7d** and **8d** showed a moderate activity with EC₅₀ values of 67.8 ± 0.7 and 74.8 ± 0.6 μM, respectively.

Considering the data listed in Table 1, a brief structure–activity relationship can be presented for benzyl-1,2,3-triazole-linked 5-benzylidene (thio)barbiturates as free-radical scavengers. Generally, compounds bearing a chloro (compound **7a**) or a fluoro (compounds **8f** and **8h**) group on benzyl-triazole moiety showed a greater free-radical scavenging activity than compounds having a hydrogen or a bromo substitution. The introduction of bromo or methyl substituent on benzylidene moiety, as in **8g** and **8h** in comparison with their counterparts **8d** and **8f**, would reduce

the activity. Comparing EC_{50} values of **8d** and **8e** with **8a** and **8b**, respectively, it can be deduced that thiobarbiturates were better radical scavengers than their barbiturate counterparts.

2.3.3 | Determining the inhibitory mechanism on mushroom tyrosinase

The most potent tyrosinase inhibitor, derivative **8h**, was selected to determine its inhibition type on mushroom tyrosinase diphenolase activity. The kinetic studies of the enzyme by the Lineweaver–Burk plot of $1/V$ versus $1/[S]$ in the presence of different inhibitor concentrations gave a series of straight lines intersected within the second quadrant, as shown in Figure 2. With the increase in the concentration of **8h**, there was an increase in K_m values and a decrease in V_m values. The result indicated that **8h** inhibits tyrosinase by two different pathways: competitively forming enzyme–inhibitor complex and interrupting enzyme–substrate–inhibitor complex in a noncompetitive manner. Therefore, it could be stated that **8h** was a mixed-type tyrosinase inhibitor. The equilibrium constants for its binding with free enzyme, K_I , and with the enzyme–substrate complex, K_{IS} , were determined from the second plots of K_m/V_m and $1/V_m$ versus the concentration of **8h**, respectively. The values of K_I and K_{IS} were calculated to be 60.27 and 143.51 μM , respectively.

2.4 | Molecular docking study

To inquire about the binding mode and potential interactions of presented tyrosinase inhibitors at the active site of tyrosinase

enzyme, a molecular docking analysis was carried out. Docking results and binding affinities of the enzyme–inhibitor complexes are listed in Table 2. The more negative estimated free energy of binding (ΔG) indicated the more stable complex that was formed between the ligand and target enzyme. The docking results are in good agreement with the experimental outcomes. Docking studies indicated that all the active derivatives were well accommodated within the tyrosinase binding pocket with binding energy values ranging from -6.95 to -8.81 kcal/mol. The most active benzyl-1,2,3-triazole-linked 5-benzylidene (thio)barbiturate derivatives **8b** and **8h** possessed the most negative binding energy values of -8.55 and -8.81 kcal/mol, respectively.

The binding poses and interactions of **8b** and **8h** at the binding site of mushroom tyrosinase are depicted in Figures 3a and 3b, respectively. The pyrimidine-trione ring in **8b** compound and the thioxo-dihydropyrimidine-dione ring of derivative **8h** were similarly oriented in the enzyme active site so that the two rings formed three key hydrogen bonds with His85, Asn81, and Glu322, and also one Pi-H interaction with His85. However, the presence of different substituents on phenyl rings caused other moieties of **8a** and **8h** to have dissimilar orientations. The triazole ring in compound **8a** formed a hydrogen bond with Ser282 residue and 4-Br substituent interacted with copper ions; however, in the case of **8h**, the triazole core formed a hydrogen bond with His244 and 4-fluorophenyl ring participated in a Pi-alkyl interaction with Val283.

From the docking results presented in Table 2, it can be stated that the orientations of pyrimidine-trione and thioxo-dihydropyrimidine-dione rings, and their ability to form hydrogen bonds with Asn81 and Glu322 had a significant role in the inhibitory potency of these compounds. In the case of the less potent tyrosinase

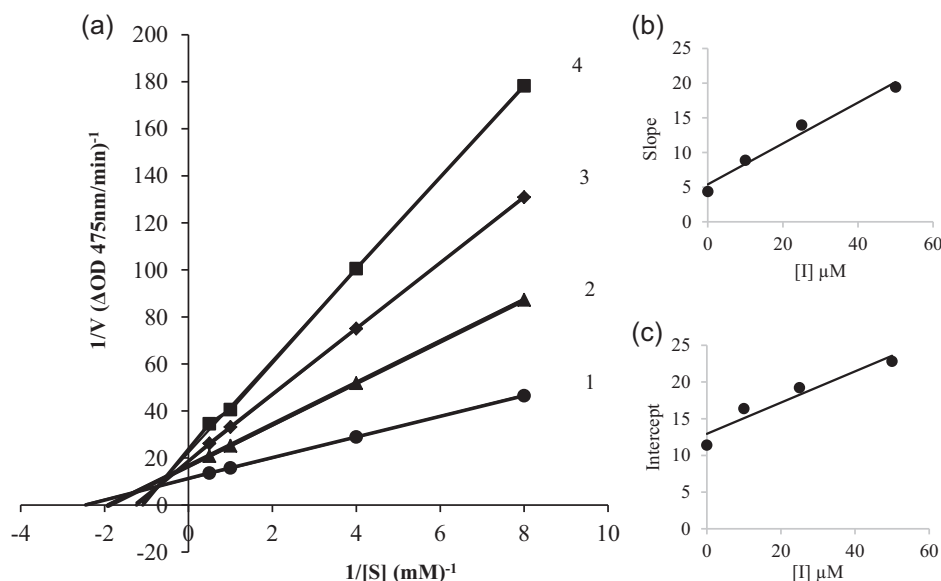
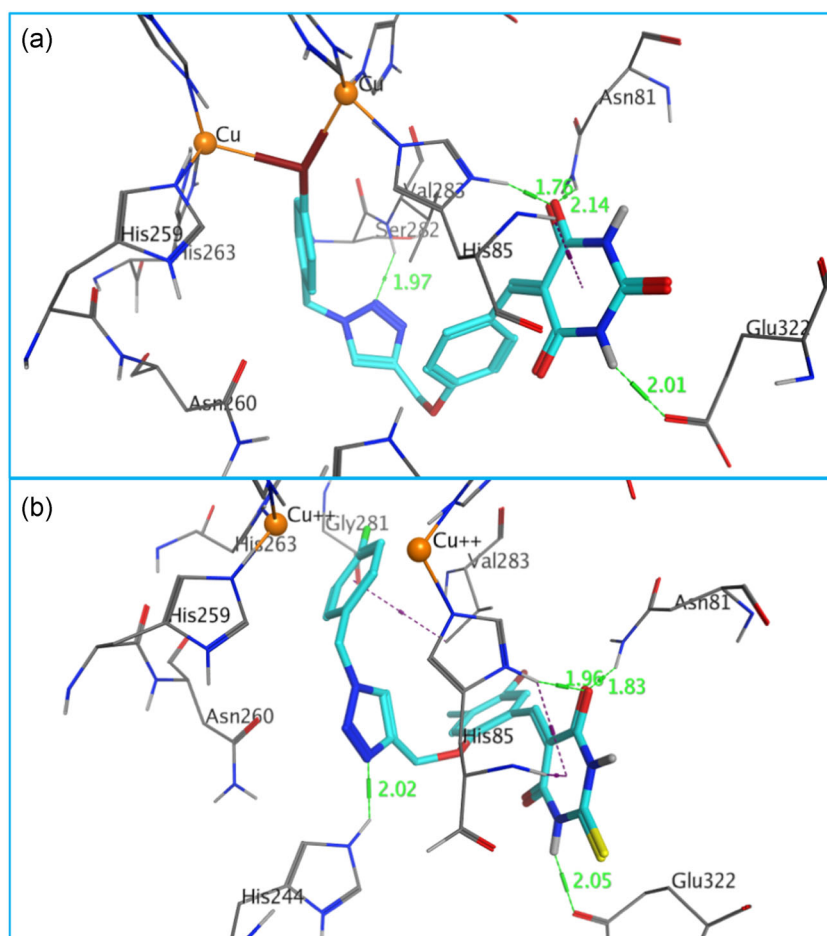


FIGURE 2 (a) Lineweaver–Burk plots for tyrosinase inhibition in the presence of **8h** as an inhibitor and L-DOPA as a substrate. The reciprocal tyrosinase inhibitory activity was plotted against the reciprocal substrate concentration (double-reciprocal plot, $n = 3$). Concentrations of **8h** for curves 1–4 were 0, 10, 25, and 50 μM , respectively. (b, c) Plots of slope and intercept versus concentration of **8h** for determining the inhibition constants K_I and K_{IS} , respectively

TABLE 2 Docking results of the suggested tyrosinase inhibitors at the tyrosinase binding site

Code	ΔG (kcal/mol)	K_i (μM)	Interactions	Atom of ligand	Amino acid	Distance (\AA)
8a	-6.95	8.07	Pi-alkyl	Phenyl ring	Val283	
			Pi-H	Pyrimidine-trione ring	His244	
8b	-8.55	0.54	H-bonding	C=O of pyrimidine-trione ring	His85	1.76
			H-bonding	C=O of pyrimidine-trione ring	Asn81	2.14
			H-bonding	N-H of pyrimidine-trione ring	Glu322	2.01
			H-bonding	N of triazole ring	Ser282	1.97
				Br	Cu	2.83
				Br	Cu	2.90
			Pi-H	Pyrimidine-trione ring	His85	
8d	-7.78	1.97	H-bonding	N-H of thioxo-dihydropyrimidine-dione	His244	1.81
			H-bonding	C=S of thioxo-dihydropyrimidine-dione	His85	3.16
8e	-8.15	1.07	H-bonding	N-H of thioxo-dihydropyrimidine-dione	His244	1.81
			H-bonding	C=S of thioxo-dihydropyrimidine-dione	His85	3.07
				Br	Cu	2.58
				Br	Cu	2.64
8h	-8.81	0.35	H-bonding	C=S of thioxo-dihydropyrimidine-dione	His85	1.96
			H-bonding	C=S of thioxo-dihydropyrimidine-dione	Asn81	1.83
			H-bonding	N-H of thioxo-dihydropyrimidine-dione	Glu322	2.05
			H-bonding	N of triazole ring	His244	2.02
			Pi-H	Thioxo-dihydropyrimidine-dione	His85	
			Pi-H	Thioxo-dihydropyrimidine-dione	His85	
			Pi-alkyl	4-Fluorophenyl ring	Val283	

**FIGURE 3** The binding orientation of (a) **8b** and (b) **8h** within the active site of tyrosinase enzyme (PDB: 2Y9X). The inhibitors and amino acids are displayed as cyan and gray sticks, respectively

inhibitors **8d** and **8e**, the thioxo-dihydropyrimidine-dione formed two hydrogen bonds with His85 and His244, but the other two key hydrogen bonds with Asn81 and Glu322 were not observed. The least potent inhibitor **8a** possessed the least favorable binding energy. Moreover, the orientation of **8a** was very different from that of the other compounds and the pyrimidine-trione ring formed no hydrogen-bonding interaction with the active site residues.

3 | CONCLUSIONS

The 5-benzylidene (thio)barbiturate-1,2,3-triazole hybrids bearing different benzyl moieties were designed according to the structures of 4-methoxybenzylidene (thio)barbiturate derivatives and phthalimide-triazole hybrid analogs reported in the literature as tyrosinase inhibitors. The compounds were synthesized to evaluate their tyrosinase inhibitory activity and DPPH free-radical scavenging potential. Two derivatives, **8h** and **8b**, showed a promising inhibitory effect on the tyrosinase diphenolase activity ($IC_{50} = 24.6 \pm 0.9$ and $26.8 \pm 0.8 \mu M$, respectively). The compounds exhibited a better tyrosinase inhibitory activity than each of their primary components, based on which they were designed. Most of the compounds exhibited a good radical scavenging activity; however, **7a**, **8f**, and **8h** were the most potent derivatives with EC_{50} values of 29.9 ± 0.8 , 36.8 ± 0.9 , and $39.2 \pm 1.1 \mu M$, respectively. The kinetic analysis showed that compound **8h** was a mixed-type tyrosinase inhibitor. Docking analysis results of the derivatives showed that the tyrosinase inhibitory activity was in agreement with the biological evaluation. **8b** and **8h** possessed the most negative binding energy values of -8.55 and -8.81 kcal/mol, respectively. Moreover, it was found that the Asn81 and Glu322 amino acids played a significant role in forming stable enzyme-inhibitor complexes. Consequently, compound **8h** could be a promising lead with dual biological activities as a potent tyrosinase inhibitor and a potential antioxidant in the field of drug discovery, and further development of such a compound in cosmetics, medicine, or food industry may be of interest.

4 | EXPERIMENTAL

4.1 | Chemistry

4.1.1 | General

All reagents and solvents were purchased from commercial suppliers. Mushroom tyrosinase (EC1.14.18.1), kojic acid, DMSO, L-DOPA, and DPPH were purchased from Sigma Chemical Co. (St. Louis, MO). Melting points were measured on a Kofler hot-stage apparatus and were uncorrected. The nuclear magnetic resonance spectra were recorded on a Bruker DRX-400 Avance instrument (400.1 MHz for 1H , 100.6 MHz for ^{13}C) using DMSO as the solvent. The infrared (IR) spectra were recorded on an FT-IR Bruker Vector 22 spectrometer. The mass spectra were recorded on a Finnigan MAT 8430 mass spectrometer

operating at an ionization potential of 70 eV. Elemental analyses were realized using a PerkinElmer 2400II CHNS/O elemental analyzer.

The InChI codes of the investigated compounds, together with some biological activity data, are provided as Supporting Information Data.

4.1.2 | Synthesis

All triazoles incorporating barbituric motifs were prepared according to the described procedure.^[35]

4.1.3 | Propargylation of hydroxybenzaldehyde derivatives 2a-d

Propargyl bromide (6 mmol) was added to a stirred solution of corresponding hydroxybenzaldehydes **1a**, **1b**, **1c**, or **1d** (5 mmol) and potassium carbonate (5 mmol) in DMF (15 ml). The mixture was stirred for 4–24 hr, water was added, and the precipitate was filtered and washed with water.

4.1.4 | General procedure for the preparation of 5-[prop-2-yn-1-yloxy]benzylidene] (thio) barbiturates 4a-f

5-[4-(Prop-2-yn-1-yloxy)benzylidene]pyrimidine-2,4,6(1H,3H,5H)-trione (**4a**), 5-[2-(prop-2-yn-1-yloxy)benzylidene]pyrimidine-2,4,6(1H,3H,5H)-trione (**4b**), 5-[5-bromo-2-(prop-2-yn-1-yloxy)benzylidene]pyrimidine-2,4,6(1H,3H,5H)-trione (**4c**), 5-[2-(prop-2-yn-1-yloxy)benzylidene]-2-thioxodihydropyrimidine-4,6(1H,5H)-dione (**4d**), and 5-[5-bromo-4-methyl-2-(prop-2-yn-1-yloxy)benzylidene]-2-thioxodihydropyrimidine-4,6(1H,5H)-dione (**4e**):

Propargylated aldehydes **2a-d** (1 mmol) were added to a stirred solution of (thio)barbituric acid **3a,b** (1.2 mmol) in aqueous HCl (25 ml, 10%; 1.0 mmol) at room temperature. After the mixture was stirred for 2–10 hr, the precipitated material was filtered and washed with water and ethanol.

1,3-Dimethyl-5-[4-(prop-2-yn-1-yloxy)benzylidene]pyrimidine-2,4,6(1H,3H,5H)-trione (**4f**):

Propargylated aldehyde **2b** (1.0 mmol) was added to a stirred solution of *N,N*-dimethylbarbituric acid (**3c**, 1.2 mmol) in water (20 ml) containing $(NH_4)_2HPO_4$ (20 mol%) at room temperature. After stirring the mixture for 4–12 hr, the yellow precipitate was filtered and washed with water and ethanol.

4.1.5 | General procedure for the preparation of alkyl azides; 1-(azidomethyl)-2-chlorobenzene (**6a**), 1-(azidomethyl)-4-bromobenzene (**6b**), (azidomethyl) benzene (**6c**), 1-(azidomethyl)-4-fluorobenzene (**6d**)

Sodium azide (1.2 mmol) was added to a solution of the required benzyl bromide derivative **5a-d** (1 mmol) in DMF. The mixture was

heated at 100°C, and after completion of the reaction (3 hr), the reaction mixture was quenched with an aqueous solution of NH₄Cl (15 ml) and extracted with ethyl acetate (3 × 20 ml). The combined organic extracts were washed with brine (3 × 20 ml) and dried over MgSO₄. After evaporation of the solvent at reduced pressure, the pure azides were isolated.

4.1.6 | General procedure for the preparation of 7a–d and 8a–h

Alkynes **4a–f** (1.2 mmol) and benzyl azide **6a–d** (1 mmol) were added to a solution of CuSO₄ (0.2 equiv.) in DMSO (10 ml) in a capped flask at room temperature. The reaction mixture was stirred at 80°C, and after completion of the reaction (12 hr), the reaction mixture was quenched with a saturated aqueous solution of NH₄Cl (30 ml) and extracted with ethyl acetate (3 × 40 ml). The combined organic extracts were washed with brine (3 × 30 ml), dried over Na₂SO₄, and concentrated under vacuum.

The spectroscopic characterization of compounds **7a,b**, **8a–e**, and **8g,h** is provided as Supporting Information Data.

4.2 | Biological evaluations

4.2.1 | Mushroom tyrosinase inhibition assay

Mushroom tyrosinase was assayed as reported in our previous studies.^[36–38] L-DOPA was used as the substrate and enzyme activity was checked by detecting dopachrome formation at 475 nm. All test samples were dissolved in DMSO at 40 mM and diluted to the required concentrations. First, 10 ml of tyrosinase (0.5 mg/ml) was mixed with 160 ml of phosphate buffer (50 mM, pH 6.8) in 96-well microplates, and then 10 ml of the test sample was added. The plates were incubated at 28°C for 20 min, and then 20 ml of L-DOPA solution (0.5 mM) was added to the phosphate buffer. Each concentration was analyzed in three independent experiments run in triplicate. The inhibitory activity of the tested compounds was expressed as the concentration that inhibited 50% of the enzyme activity (IC₅₀). The percent inhibition ratio was calculated according to the following equation:

$$\text{Inhibition (\%)} = 100 \times [(\text{Abs}_{\text{control}} - \text{Abs}_{\text{compound}}) / \text{Abs}_{\text{control}}].$$

4.2.2 | DPPH free-radical scavenging assay

The samples were dissolved in DMSO at 40 mM and diluted to the required concentrations. A mixture of test compound and DPPH solution (110 μM in methanol) was shaken in the dark at room temperature for 30 min. The mixture absorbance was measured at 517 nm. The DPPH solution without test compounds was used as the control and quercetin was used as the positive control. The percentage of free-radical scavenging activity was calculated as follows:

$$\text{Radical scavenging activity (\%)} = 100 \times [(\text{Abs}_{\text{control}} - \text{Abs}_{\text{compound}}) / \text{Abs}_{\text{control}}].$$

The EC₅₀ values were calculated from a linear regression plot between the test compounds' concentrations and percent radical scavenging activity. Each concentration was analyzed in three independent experiments run in triplicate.

4.2.3 | Inhibitory mechanism of 8h on the diphenolase activity of mushroom tyrosinase

A series of experiments was performed to determine the inhibition kinetics of **8h**. The inhibitor concentrations were 0, 10, 25, and 50 μM. Substrate (L-DOPA) concentrations were 0.125, 0.250, 1.000, and 2.000 mM in all kinetic studies. Pre-incubation and measurement time were the same as described in the tyrosinase inhibition assay procedure. The tyrosinase inhibition type was then calculated using Lineweaver–Burk plots of inverse velocities (1/V) versus inverse substrate concentrations, 1/[S] mM. The Michaelis constant (K_m) and maximal velocity (V_m) were calculated by Lineweaver–Burk plots and the inhibition constants were determined by the second plot of apparent K_m/V_m or 1/V_m versus the concentration of the inhibitor.

4.3 | Molecular docking study

Docking was performed by AutoDock 4.2 and AutoDock Tools 1.5.4 (ADT). The X-ray crystal structure of *Agaricus bisporus* tyrosinase containing tropolone as the co-crystallized ligand in the binding site (PDB ID: 2Y9X) was taken from Protein Data Bank (<http://www.rcsb.org>). Before the docking analysis, tropolone and water molecules were omitted from 2Y9X, and then hydrogens were added and nonpolar hydrogens were merged. Finally, Gasteiger charges were calculated for the protein. The three-dimensional structures of ligands were sketched and minimized using HyperChem software. PDBQT formats of the ligands were prepared. The grid maps were constructed by AutoGrid and grid box dimensions were set to 40 × 40 × 40 with 0.375-Å grid spacing. The active site that comprises copper metal ions was selected for docking and the grids' centers were placed on the tropolone's binding site. For the docking parameter file, rigid macromolecule and Lamarckian genetic search algorithm were chosen. The number of GA runs was set at 100 and other parameters were left at program default values.

ACKNOWLEDGMENTS

The authors wish to thank the Vice-Chancellor for Research, Shiraz University of Medical Sciences, Iran (project numbers: 95-01-103-12178 and 98-01-36-20126).

CONFLICT OF INTERESTS

The authors declare that there are no conflicts of interests.

ORCID

Mehdi Khoshneviszadeh  <http://orcid.org/0000-0003-1458-2964>

REFERENCES

- [1] S.-Y. Seo, V. K. Sharma, N. Sharma, *J. Agric. Food Chem.* **2003**, 51, 2837.
- [2] S. H. Pomerantz, *J. Biol. Chem.* **1966**, 241, 161.
- [3] M. N. Masum, K. Yamauchi, T. Mitsunaga, *Rev. Agric. Sci.* **2019**, 7, 41.
- [4] T. Pillaiyar, M. Manickam, V. Namasivayam, *J. Enzyme Inhib. Med. Chem.* **2017**, 32, 403.
- [5] T. Hasegawa, *Int. J. Mol. Sci.* **2010**, 11, 1082.
- [6] M. Loizzo, R. Tundis, F. Menichini, *Compr. Rev. Food Sci. Food Saf.* **2012**, 11, 378.
- [7] S. H. Bang, S. J. Han, D. H. Kim, *J. Cosmet. Dermatol.* **2008**, 7, 189.
- [8] Z.-M. Hu, Q. Zhou, T.-C. Lei, S.-F. Ding, S.-Z. Xu, *J. Dermatol. Sci.* **2009**, 55, 179.
- [9] T.-S. Chang, *Int. J. Mol. Sci.* **2009**, 10, 2440.
- [10] H. M. Faidallah, K. A. Khan, *J. Fluorine Chem.* **2012**, 142, 96.
- [11] Y.-C. Jeong, M. Moloney, *Molecules* **2015**, 20, 3582.
- [12] S. R. Whittle, A. J. Turner, *Biochem. Pharmacol.* **1982**, 31, 2891.
- [13] F. López-Muñoz, R. Ucha-Udabe, C. Alamo, *Neuropsychiatr. Dis. Treat.* **2005**, 1, 329.
- [14] J. S. Lundy, *Anesth. Analg.* **1929**, 8, 360.
- [15] D. Kalaivani, R. Malarvizhi, R. Subbalakshmi, *Med. Chem. Res.* **2008**, 17, 369.
- [16] N. R. Penthal, A. Ketkar, K. R. Sekhar, M. L. Freeman, R. L. Eoff, R. Balusu, P. A. Crooks, *Bioorg. Med. Chem.* **2015**, 23, 7226.
- [17] P. Bhatt, M. Kumar, A. Jha, *ChemistrySelect* **2018**, 3, 7060.
- [18] N. R. Penthal, P. R. Ponugoti, V. Kasam, P. A. Crooks, *Bioorg. Med. Chem. Lett.* **2013**, 23, 1442.
- [19] K. M. Khan, M. Ali, A. Wadood, M. Khan, M. A. Lodhi, S. Perveen, M. I. Choudhary, W. Voelter, *J. Mol. Graphics Modell.* **2011**, 30, 153.
- [20] S. V. Laxmi, Y. T. Reddy, B. S. Kuarm, P. N. Reddy, P. A. Crooks, B. Rajitha, *Bioorg. Med. Chem. Lett.* **2011**, 21, 4329.
- [21] B. B. Sokmen, S. Ugras, H. Y. Sarikaya, H. I. Ugras, R. Yanardag, *Appl. Biochem. Biotechnol.* **2013**, 171, 2030.
- [22] Q. Yan, R. Cao, W. Yi, L. Yu, Z. Chen, L. Ma, H. Song, *Bioorg. Med. Chem. Lett.* **2009**, 19, 4055.
- [23] Z. Chen, D. Cai, D. Mou, Q. Yan, Y. Sun, W. Pan, Y. Wan, H. Song, W. Yi, *Bioorg. Med. Chem.* **2014**, 22, 3279.
- [24] Q. Yan, R. Cao, W. Yi, Z. Chen, H. Wen, L. Ma, H. Song, *Eur. J. Med. Chem.* **2009**, 44, 4235.
- [25] C. H. Zhou, Y. Wang, *Curr. Med. Chem.* **2012**, 19, 239.
- [26] M. Gholampour, S. Ranjbar, N. Edraki, M. Mohabbati, O. Firuzi, M. Khoshneviszadeh, *Bioorg. Chem.* **2019**, 88, 102967.
- [27] R. Kant, D. Kumar, D. Agarwal, R. D. Gupta, R. Tilak, S. K. Awasthi, A. Agarwal, *Eur. J. Med. Chem.* **2016**, 113, 34.
- [28] S. Haider, M. S. Alam, H. Hamid, S. Shafi, A. Nargotra, P. Mahajan, S. Nazreen, A. M. Kalle, C. Kharbanda, Y. Ali, *Eur. J. Med. Chem.* **2013**, 70, 579.
- [29] N. Fu, S. Wang, Y. Zhang, C. Zhang, D. Yang, L. Weng, B. Zhao, L. Wang, *Eur. J. Med. Chem.* **2017**, 136, 596.
- [30] Y. Sajja, S. Vanguru, H. R. Vulupala, R. Bantu, P. Yogeswari, D. Sriram, L. Nagarapu, *Bioorg. Med. Chem. Lett.* **2017**, 27, 5119.
- [31] M. Mohammadi-Khanaposhtani, M. Saeedi, N. S. Zafarghandi, M. Mahdavi, R. Sabourian, E. K. Razkenari, H. Alinezhad, M. Khanavi, A. Foroumadi, A. Shafiee, *Eur. J. Med. Chem.* **2015**, 92, 799.
- [32] M. B. Tehrani, P. Emani, Z. Rezaei, M. Khoshneviszadeh, M. Ebrahimi, N. Edraki, M. Mahdavi, B. Larijani, S. Ranjbar, A. Foroumadi, *J. Mol. Struct.* **2019**, 1176, 86.
- [33] M. Mahdavi, A. Ashtari, M. Khoshneviszadeh, S. Ranjbar, A. Dehghani, T. Akbarzadeh, B. Larijani, M. Khoshneviszadeh, M. Saeedi, *Chem. Biodiversity* **2018**, 15, e1800120.
- [34] K. M. Khan, M. Ali, A. Ajaz, S. Perveen, M. I. Choudhary, *Lett. Drug. Des. Discov.* **2008**, 5, 286.
- [35] M. Darroudi, Y. Sarrafi, M. Hamzehloueian, *J. Serb. Chem. Soc.* **2018**, 83, 821.
- [36] S. Ranjbar, A. Akbari, N. Edraki, M. Khoshneviszadeh, H. Hemmatian, O. Firuzi, M. Khoshneviszadeh, *Lett. Drug. Des. Discov.* **2018**, 15, 1170.
- [37] Z. Dehghani, M. Khoshneviszadeh, M. Khoshneviszadeh, S. Ranjbar, *Bioorg. Med. Chem.* **2019**, 27, 2644.
- [38] S. Ghafari, S. Ranjbar, B. Larijani, M. Amini, M. Biglar, M. Mahdavi, M. Bakhshaei, M. Khoshneviszadeh, A. Sakhteman, M. Khoshneviszadeh, *Int. J. Biol. Macromol.* **2019**, 135, 978.

SUPPORTING INFORMATION

Additional supporting information may be found online in the Supporting Information section.

How to cite this article: Ranjbar S, Shahvaran P-s, Edraki N, et al. 1,2,3-Triazole-linked 5-benzylidene (thio)barbiturates as novel tyrosinase inhibitors and free-radical scavengers. *Arch Pharm.* 2020;e2000058.

<https://doi.org/10.1002/ardp.202000058>